MITSUBISHI ELECTRIC RESEARCH LABORATORIES
http://www.merl.com

Model Predictive Control of Vapor Compression Systems

Jain, N.; Burns, D.J.; Di Cairano, S.; Laughman, C.R.; Bortoff, S.A.

TR2014-075 July 2014

Abstract

Model Predictive Control (MPC) of vapor compression systems (VCSs) offers several advantages over conventional control methods (such as multivariable process control with selector logic) in terms of 1) the resulting closed-loop performance and 2) the control engineering design process. VCSs are multivariable systems and feature constraints on system variables and actuators that must be enforced during steady-state and transient operation. We present the design and validation of an MPC for a split ductless VCS. The design regulates room temperature with zero steady state error for unknown changes in the thermal load and enforces constraints on system variables such as compressor discharge temperature and actuator ranges and rates. We show how the MPC design can evolve during the engineering process by adding and modifying constraints and process variables. The design methodology provides guarantees in terms of closed loop stability and convergence. Importantly, in contrast to other published results on MPC for VCSs, our design makes use of only available temperature measurements and does not require pressure or mass flow measurements which are typically not available in production VCSs.

International Refrigeration and Air Conditioning Conference at Purdue

Model Predictive Control of Vapor Compression Systems

Neera JAIN, Daniel J. BURNS*, Stefano DI CAIRANO, Christopher R. LAUGHMAN, Scott A. BORTOFF

Mitsubishi Electric Research Laboratories,
Cambridge, MA, USA
burns@merl.com

* Corresponding Author

ABSTRACT

Model Predictive Control (MPC) of vapor compression systems (VCSs) offers several advantages over conventional control methods (such as multivariable process control with selector logic) in terms of 1) the resulting closed-loop performance and 2) the control engineering design process. VCSs are multivariable systems and feature constraints on system variables and actuators that must be enforced during steady-state and transient operation. We present the design and validation of an MPC for a split ductless VCS. The design regulates room temperature with zero steady state error for unknown changes in the thermal load and enforces constraints on system variables such as compressor discharge temperature and actuator ranges and rates. We show how the MPC design can evolve during the engineering process by adding and modifying constraints and process variables. The design methodology provides guarantees in terms of closed loop stability and convergence. Importantly, in contrast to other published results on MPC for VCSs, our design makes use of only available temperature measurements and does not require pressure or mass flow measurements which are typically not available in production VCSs.

1. INTRODUCTION

Model Predictive Control (MPC) (Garcia et al., 1989) of vapor compression systems (VCSs) offers several advantages over conventional control methods (such as multivariable process control with selector logic) in terms of 1) the resulting closed-loop performance and 2) the control engineering design process. VCSs are multivariable systems and feature constraints on system variables and actuators that must be enforced during steady-state and transient operation. Control requirements typically include regulation of process variables such as room temperatures, high bandwidth transient response for rapid pull down, constraint enforcement during transient and steady-state operation, and optimal steady-state energy efficiency. Conventional methods of control use classical or multivariable process control theory to meet the requirements associated with regulation, transient response, and steady-state efficiency, together with selector logic designed to prioritize the process variables in order to enforce constraints (Amano, 2012). However, for multivariable systems with more than one constraint, the interactions among the selector logic make it difficult to design and validate the feedback controller; feedback gains are often detuned resulting in a conservative feedback controller that is intended to *stay away* from the constraints. At best, this results in slow transient response and poor rejection of disturbances and at worst, in a controller that is unable to maintain the system within the constraints.

In contrast, MPC is a technology that is well suited to the requirements of VCS control. Elliott and Rasmussen (2008) and Koeln and Alleyne (2013) investigate decentralized MPC for multi-evaporator VCSs to regulate evaporator superheat and cooling capacity while mitigating coupling between individual evaporators. However, evaporator superheat and cooling capacity are feedback variables that may require pressure or mass flow measurements which are typically not available in production VRF systems. To overcome model uncertainty between a linear MPC and the nonlinear VCS, Wallace et al. (2012) use a state estimator with an input disturbance model that results in zero steady-state regulation error. Heuristic tuning guidelines are provided for the input disturbance model. Like Elliott and Rasmussen (2008), Wallace et al. (2012) use MPC to control the *cooling capacity* of the VCS, while a supervisory controller is used to determine appropriate setpoints to regulate zone temperature(s).

However, when considering zone temperature rather than cooling capacity as a feedback variable, the unknown and unmeasurable thermal loads on the VCS are disturbances that must be rejected by the MPC. Our approach is to formulate the state estimator in such a way that the effect of disturbances are lumped into auxiliary output disturbance states, thereby eliminating the need to measure the thermal load. This approach has the added benefit of offset-free estimation (Pannocchia and Rawlings, 2003; Maeder et al., 2009) of all measured outputs. This means that our closed-loop system will achieve zero steady-state error between set point variables and regulated variables for constant but unmeasured and unknown values of the thermal load disturbance. Moreover, we show that MPC offers a flexible and systematic design process in which the constraints, for example, can be modified as the design evolves, and the resulting controller can be computed and analyzed immediately, providing rigorous guarantees on optimality, transient performance, and stability.

The paper is organized as follows. Section 2 describes the nonlinear model of a single zone split ductless vapor compression system and its linearization for controller design. The design of the MPC is presented in Section 3 and simulation results showing the performance and capabilities of the controller are presented and discussed in Section 4. Concluding remarks are offered in Section 5.

2. SYSTEM MODELING

A nonlinear dynamic model of a 2.6 kW capacity split ductless VCS is developed using the THERMOSYS Toolbox for MATLAB/Simulink (Alleyne, 2012). THERMOSYS uses a lumped parameter moving boundary approach for modeling the dynamics of the heat exchangers. The system-level model contains component models of the condenser, electronic expansion valve (EEV), evaporator, and the compressor, as well as a model of the zone that is interacting with the VCS. Disturbances from thermal loads and changes in the outdoor air temperature are included in the nonlinear model.

The MPC state estimator and constrained optimizer used in this approach both require linear models. The chosen constrained optimizer, a parallel quadratic programming (PQP) algorithm (Di Cairano et al., 2013a), is motivated by its execution speed and convergence guarantee. Therefore, the nonlinear model VCS model is linearized around a 2.6 kW load operating point. Individual open-loop step responses are collected between the control inputs and the measured outputs (Table 1) in simulation. Transfer functions are fit to each of the open loop step responses and combined into a transfer function matrix that is subsequently approximated using the optimal Hankel norm model order reduction technique (Skogestad and Postlethwaite, 2005). The resulting sixth-order continuous linear time-invariant model of the VCS is written in state space form as

$$\begin{aligned} \dot{x}(t) &= Ax(t) + Bu(t) \\ y_m(t) &= Cx(t), \end{aligned} \tag{1}$$

where $x(t)$ are the dynamic states, $y_m(t)$ are the measured outputs, and $u(t)$ are the controlled inputs. Note that the states of the model may not have physical significance due to the model reduction procedure as well as the empirical nature of the identified transfer functions.

Table 1: DEFINITION OF SIGNALS

Signal Type	Signal Symbol	Signal Description	Units
Control Input	u_1	compressor frequency	Hz
	u_2	EEV aperture	counts
	u_3	condenser fan speed	rpm
Measured Output	y_{m1}	compressor discharge temperature	°C
	y_{m2}	compressor discharge superheat temperature	°C
	y_{m3}	evaporating temperature	°C
	y_{m4}	room air temperature	°C

Thermal load disturbances are not included in the linearized model because in general, these disturbances are difficult to measure or predict. Furthermore, in some controller designs, the evaporator fan speed may be considered a con-

trol input and included in a straightforward manner. However, in the design that we consider, the evaporator fan is controlled by the occupant and its influence may instead be considered as a measured disturbance. Specifically, the evaporator fan speed will be fixed at a constant value in this design.

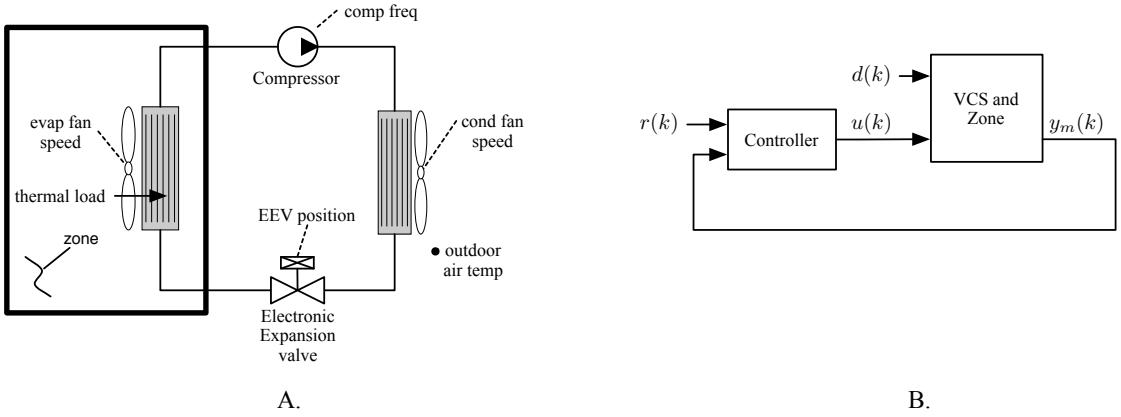

Figure 1: (A) VCS schematic and (B) Block diagram of controller interacting with the VCS and Zone.

3. CONTROLLER DESIGN

A schematic of the online implementation of the controller is shown in Figure 2. The controller consists of two elements: i) a state estimator and ii) an MPC. In this section we discuss the key design principles for both of these elements and highlight how they provide a flexible and systematic methodology for modifying and iterating on the design.

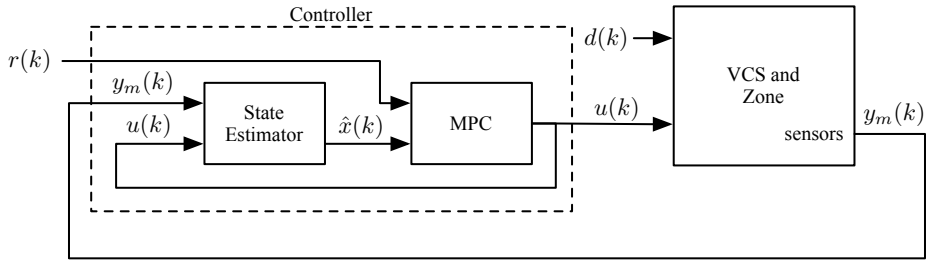

Figure 2: Block diagram describing the VCS controller.

3.1 State Estimator Design

The MPC algorithm requires an estimate of the dynamic state of the system. Estimators typically use measured output and input signals with a model of the system dynamics, Eq. (2), to estimate the dynamic states. However, when unmodeled disturbances such as changes in the thermal load act on the VCS and zone, the estimator will typically not estimate the state correctly, thereby compromising the performance of the MPC by introducing steady-state offsets between the measured and desired values of performance variables. Here we show how the effect of unmodeled disturbances and model uncertainty are captured by the addition of auxiliary output disturbance states in the estimation model. The continuous-time dynamics in Eq. (1) are discretized with a sample time of Ts_e, resulting in the discrete-time system

$$\begin{aligned} x(k+1) &= A_e x(k) + B_e u(k) \\ y_m(k) &= C_e x(k), \end{aligned} \tag{2}$$

where k is the sampling index. The set of measured outputs y_m is divided into two (potentially overlapping) subsets: performance outputs and constrained outputs. The MPC relies on a prediction model to determine the optimal control inputs that achieve offset-free tracking of the performance outputs and to guarantee that the constrained outputs stay within their bounds in the presence of unmodeled disturbances or modeling error. This can be achieved by augmenting the estimator model with auxiliary states $w \in \mathbb{R}^{p\times 1}$, where p is the number of measured outputs in the system (Pannocchia and Rawlings, 2003; Maeder et al., 2009). Each of the auxiliary states is defined as the difference between an output as predicted by Eq. (2) and the actual measured value of the output.

The augmented estimator model takes the form

$$x(k+1) = A_e x(k) + B_e u(k) \tag{3a}$$
$$w(k+1) = Iw(k) \tag{3b}$$
$$y_m(k) = C_e x(k) + Iw(k), \tag{3c}$$

where I is the $p \times p$ identity matrix. Finally, the estimator dynamics are given by

$$\begin{bmatrix}\hat{x}(k+1)\\ \hat{w}(k+1)\end{bmatrix} = \begin{bmatrix}A_e - L_{e1}C_e & -L_{e1}\\ -L_{e2}C_e & I - L_{e2}\end{bmatrix}\begin{bmatrix}\hat{x}(k)\\ \hat{w}(k)\end{bmatrix} + \begin{bmatrix}B_e\\ 0\end{bmatrix}u(k) + \begin{bmatrix}L_{e1}\\ L_{e2}\end{bmatrix}y_m(k), \tag{4}$$

where $L_e = \begin{bmatrix}L'_{e1} & L'_{e2}\end{bmatrix}'$ is the static estimator gain which can be designed using standard Kalman filtering techniques (Simon, 2006).

3.2 MPC Design

The MPC relies on the design of a prediction model and a cost function to be minimized.

3.2.1 ***Prediction Model*** For MPC, a discrete-time model of the system dynamics is used to predict the system response over the chosen prediction horizon.

$$x(k+1) = A_{pr}x(k) + B_{pr}u(k) \tag{5a}$$
$$y_c(k) = C_{pr}x(k) \tag{5b}$$
$$y_p(k) = E_{pr}x(k) \tag{5c}$$

Equation (5) provides a state-space realization of the prediction model and is based on a discretization of the system of Eq. (1) with a sample time of Ts_{pr} such that $Ts_{pr} \geq Ts_e$. To emphasize that the discretization of the prediction model is not necessarily the same as that of the estimator model, the subscript pr is appended to the state, input, and output matrices. The output matrix C_{pr} contains those rows of C such that y_c, Eq. (5b), describes the outputs to be constrained by the MPC. Similarly, E_{pr} contains those rows of C such that y_p, Eq. (5c), describes the performance outputs that are explicitly characterized in the MPC cost function (Section 3.2.2). The structure of the prediction model allows for constrained variables and performance variables to be added or removed from the controller design, highlighting the flexibility of the MPC design process.

Multiple augmentations need to be made to Eq. (5) so that the resulting MPC problem can be solved as a constrained quadratic program (QP). First, the prediction model is augmented with the same auxiliary output disturbance states that were added to the estimator model so that the prediction model predicts the effect of control decisions on the constrained and performance outputs,

$$\begin{bmatrix}x(k+1)\\ w(k+1)\end{bmatrix} = \begin{bmatrix}A_{pr} & 0\\ 0 & I\end{bmatrix}\begin{bmatrix}x(k)\\ w(k)\end{bmatrix} + \begin{bmatrix}B_{pr}\\ 0\end{bmatrix}u(k) \tag{6a}$$
$$y_c(k) = \begin{bmatrix}C_{pr} & C_w\end{bmatrix}\begin{bmatrix}x(k)\\ w(k)\end{bmatrix} \tag{6b}$$
$$y_p(k) = \begin{bmatrix}E_{pr} & E_w\end{bmatrix}\begin{bmatrix}x(k)\\ w(k)\end{bmatrix}, \tag{6c}$$

where C_w and E_w are matrices of zeros and ones such that Eqs. (6b) and Eq. (6c) are consistent with Eq. (3c).

The second modification involves expressing the input as a discrete integrator (Di Cairano et al., 2013b). This change of variables enables constraints to be placed on the rate of change of the control input and ensures that the cost function has a minimum at zero. Furthermore, we append the constrained output vector, y_c, with $y_u = x_u$ as shown in Eq. (7c) in order to enforce constraints on the actual values of the control inputs. Let $u(k) = u(k-1) + du(k)$, $x_u(k) = u(k-1)$, and $\bar{u} = du(t)$, giving

$$\begin{bmatrix} x(k+1) \\ w(k+1) \\ x_u(k+1) \end{bmatrix} = \begin{bmatrix} A_{pr} & 0 & B_{pr} \\ 0 & I & 0 \\ 0 & 0 & I \end{bmatrix} \begin{bmatrix} x(k) \\ w(k) \\ x_u(k) \end{bmatrix} + \begin{bmatrix} B_{pr} \\ 0 \\ I \end{bmatrix} \bar{u}(k) \tag{7a}$$

$$\begin{bmatrix} y_c(k) \\ y_u(k) \end{bmatrix} = \begin{bmatrix} C_{pr} & C_w & 0 \\ 0 & 0 & I \end{bmatrix} \begin{bmatrix} x(k) \\ w(k) \\ x_u(k) \end{bmatrix} \tag{7b}$$

$$y_p(k) = \begin{bmatrix} E_{pr} & E_w & 0 \end{bmatrix} \begin{bmatrix} x(k) \\ w(k) \\ x_u(k) \end{bmatrix}. \tag{7c}$$

Finally, the state vector is augmented with the reference signal(s), i.e., the setpoints for the performance outputs: room air temperature and compressor discharge temperature. By augmenting the prediction model in this manner, the cost function (Section 3.2.2) can be designed to minimize $z = y_p - r$, the error between the measured and desired values of the performance outputs as shown in Eq. (8c). The room air temperature reference r_1 is an exogenous signal and is assumed to be constant over the prediction horizon, i.e. $r_1(k+1) = r_1(k)$. The compressor discharge temperature is defined as a linear function of the compressor frequency: $r_2(k+1) = r_2(k) + c \cdot u_2(k)$. Let $x_r = r$, giving

$$\begin{bmatrix} x(k+1) \\ w(k+1) \\ x_u(k+1) \\ x_r(k+1) \end{bmatrix} = \begin{bmatrix} A_{pr} & 0 & B_{pr} & 0 \\ 0 & I & 0 & 0 \\ 0 & 0 & I & 0 \\ 0 & 0 & 0 & I \end{bmatrix} \begin{bmatrix} x(k) \\ w(k) \\ x_u(k) \\ x_r(k) \end{bmatrix} + \begin{bmatrix} B_{pr} \\ 0 \\ I \\ B_r \end{bmatrix} \bar{u}(k) \tag{8a}$$

$$\begin{bmatrix} y_c(k) \\ y_u(k) \end{bmatrix} = \begin{bmatrix} C_{pr} & C_w & 0 & 0 \\ 0 & 0 & I & 0 \end{bmatrix} \begin{bmatrix} x(k) \\ w(k) \\ x_u(k) \\ x_r(k) \end{bmatrix} \tag{8b}$$

$$z(k) = \begin{bmatrix} E_{pr} & E_w & 0 & -I \end{bmatrix} \begin{bmatrix} x(k) \\ w(k) \\ x_u(k) \\ x_r(k) \end{bmatrix}, \tag{8c}$$

where $B_r = \left[\begin{smallmatrix} c & 0 & 0 \\ 0 & 0 & 0 \end{smallmatrix}\right]$.

3.2.2 ***Cost Function*** For any type of optimal controller, one needs to mathematically describe the quantity to be minimized or maximized. For linear MPC, it is common to design a quadratic cost function,

$$J = \bar{x}(N)' P \bar{x}(N) + \sum_{k=0}^{N-1} \bar{z}(k|t)' Q_z \bar{z}(k|t) + \bar{u}(k|t)' R \bar{u}(k|t), \tag{9}$$

where $\bar{x}(k) = \begin{bmatrix} x(k)' & w(k)' & x_u(k)' & x_r(k)' \end{bmatrix}'$, $\bar{z} = y_p - r$, $\bar{u} = u(k) - u(k-1)$, and the term $\bar{x}(N)' P \bar{x}(N)$ is the terminal cost that is included to guarantee local asymptotic stability of the model predictive controller. See the Appendix for a sketch of the proof of stability and the determination of the terminal cost weight P. The matrices Q_z and R are tunable weights that influence the transient performance of the controller by penalizing the individual terms of the cost function. Finally, the cost function is minimized such that constraints

$$\bar{y}_{\min} \leq \bar{y}(k|t) \leq \bar{y}_{\max}, \quad k = 0, \ldots, N_c \tag{10a}$$

$$\bar{u}_{\min} \leq \bar{u}(k|t) \leq \bar{u}_{\max}, \quad k = 1, \ldots, N_u \tag{10b}$$

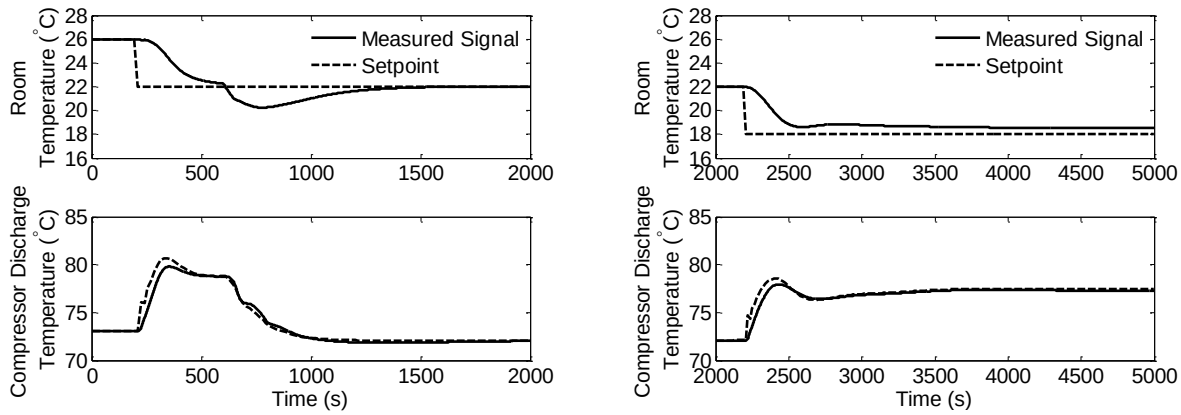

(a) t = 0 until t = 2000 seconds. **(b) t = 2000 until t = 5000 seconds.**

Figure 3: Regulation of performance variables.

are satisfied, where N_c and N_u are the time horizons over which the output and input constraints are enforced in the MPC. The prediction model, cost function, and constraints are converted into a quadratic program as described in Di Cairano and Bemporad (2010).

4. SIMULATED CASE STUDY

In order to demonstrate the advantages of MPC for VCSs, a linear MPC was designed according to the procedure outlined in the previous section and then tested on the nonlinear 2.6kW split-ductless VCS model. The outdoor air temperature is held constant at 34°C throughout the simulation. The sample time of the estimator, Ts_e, is 1 second, and the control inputs are updated at Ts_{pr} = 15 seconds. Finally, the prediction horizon has a length of 64 steps, or 16 minutes. The 5000 second simulation highlights the ability of the MPC to reject unknown thermal loads and operate the system within specified input and output constraints while still optimizing performance tracking objectives.

During the first half of the simulation from t = 0 until t = 2,000 seconds, the desired room air temperature setpoint is decreased by 4°C at t = 200 seconds; 400 seconds later, there is a 500W decrease in the thermal load acting on the room. Figures 3a, 4a, and 5a show that the controller is able to reject the disturbance and achieve steady-state offset-free tracking of the room temperature and compressor discharge temperature. Recall that the MPC does not have knowledge of the magnitude of the thermal load, but its effect on the measured outputs is estimated by the estimator. Moreover, these results show that the linear model identified based on the nonlinear model suitably represents the dynamics of the VCS.

During the second half of the simulation from t = 2,000 until t = 5,000 seconds, the desired room air temperature setpoint is decreased by another 4°C. However, at t = 1,300 seconds, the evaporating temperature constraint becomes active (see Figure 5b). The compressor speed and EEV aperture do not increase further because doing so would cause the evaporating temperature to decrease, thereby violating the constraint. Instead, the condenser fan speed decreases to drive the room air temperature as close as possible to its setpoint. Ultimately, the condenser fan speed saturates at its lower limit. Due to the enforcement of the evaporating temperature constraint and the condenser fan speed constraint, there is a steady-state offset between the room air temperature and the desired setpoint as shown in Figure 3b. This highlights how a system with more control inputs than performance outputs is advantageous in the context of MPC. With the compressor and EEV unable to drive the room air temperature to a lower value without violating the evaporating temperature constraint, the outdoor fan is able to drive the room air temperature closer to the desired value until it too reaches its lower bound (see Figure 4b). Finally, it is worth noting that the MPC enforces these competing objectives while maintaining stable operation of the VCS.

For multivariable systems (like VCSs) with complex interactions, the flexible and systematic control design process

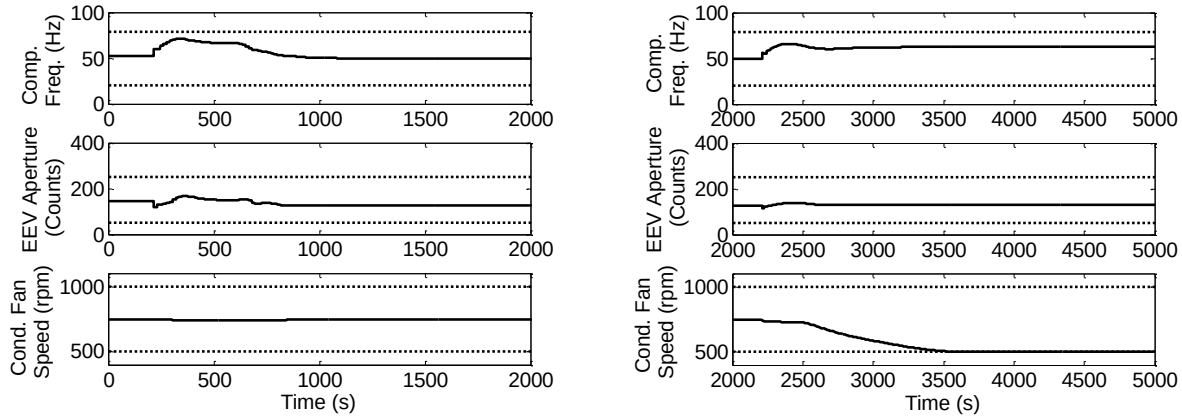

(a) t **= 0 until** t **= 2000 seconds.** **(b)** t **= 2000 until** t **= 5000 seconds.**

Figure 4: Optimal control inputs; dashed lines represent saturation bounds on each control input.

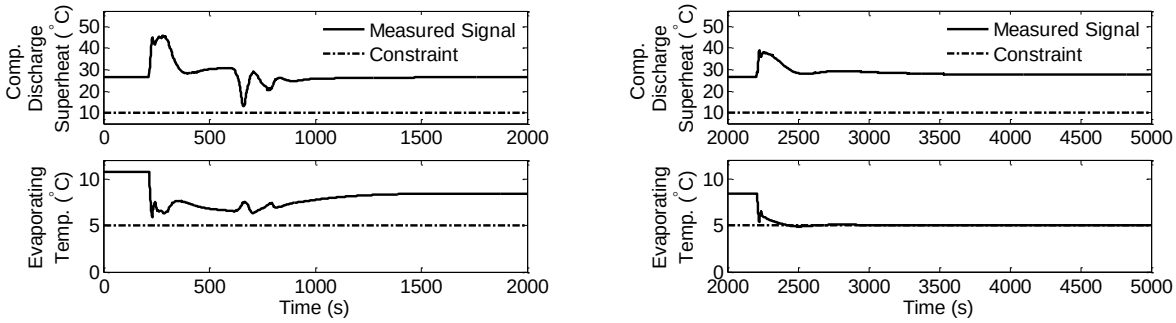

(a) t **= 0 until** t **= 2000 seconds.** **(b)** t **= 2000 until** t **= 5000 seconds.**

Figure 5: Constrained output variables.

offered by MPC is beneficial. In order to highlight this feature, the previous simulation is repeated but with a third constrained variable added to the MPC - the compressor discharge temperature. In order to make this change, only the matrix C_{pr} in Equation (5) is modified so that the vector y_c of constrained variables includes the compressor discharge temperature. The controller synthesis is otherwise unchanged.

The performance outputs y_p, control inputs u, and constrained outputs y_c for the 5000 second simulation are shown in Figures 6, 7, and 8. The MPC determines the optimal control inputs that minimize the regulation error of the performance variables (room air temperature and compressor discharge temperature) while enforcing constraints on the constrained variables. Note that the compressor discharge temperature T_d is now both a performance variable and a constrained variable. After a decrease in the room air temperature setpoint at t = 2200 seconds, both the compressor discharge temperature and evaporating temperature constraints become active, and as a result, there are steady-state offsets between the performance variables and their setpoints as shown in Figure 6. In contrast to the first simulation (Figures 3-5) the condenser fan cannot decrease to its lower bound without causing a violation of the compressor discharge temperature constraint.

5. CONCLUSION

In this paper we showed that model predictive control (MPC) of vapor compression systems (VCSs) offers several advantages over conventional control methods in terms of 1) the resulting closed-loop performance and 2) the control

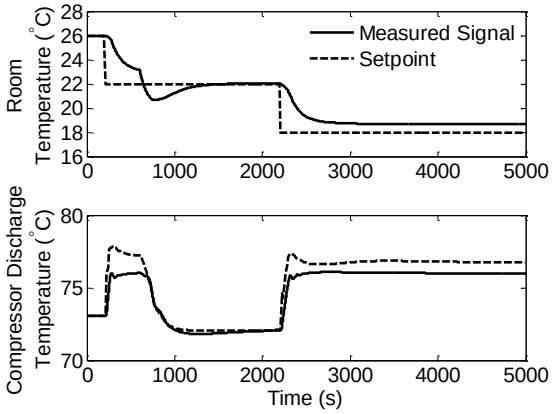

Figure 6: Sim. 2 – Regulation of performance variables.

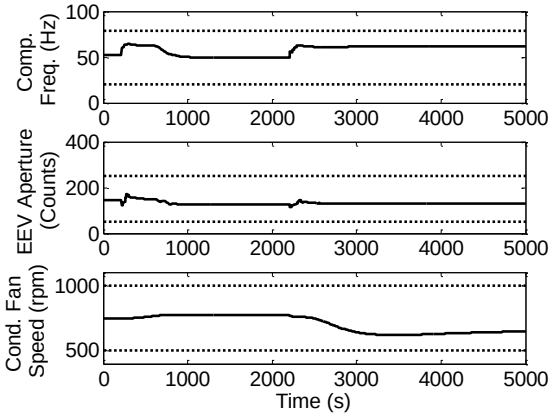

Figure 7: Sim. 2 – Optimal control inputs; dashed lines show saturation bounds.

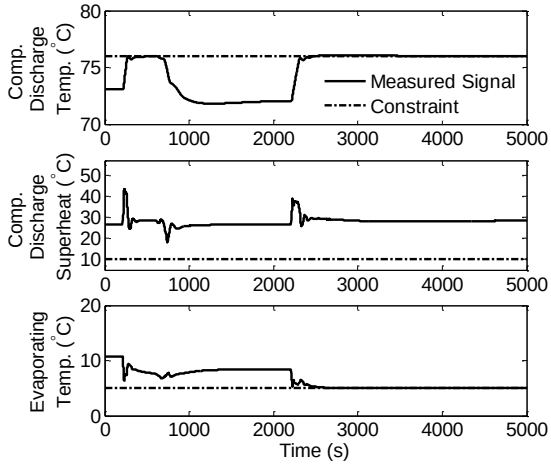

Figure 8: Simulation 2 – Constrained outputs.

engineering design process. Rather than designing multiple individual loops to address the various constraints in the system, a *single* MPC was systematically designed for the VCS with multiple control inputs, performance objectives, and constraints. Moreover, the addition or subtraction of performance objectives or constraints requires only minor changes to the state-space representation of the estimator and prediction models. Through a simulated case study it was shown that with the state estimator augmented with auxiliary output disturbance states, unmeasured thermal load disturbances are rejected in the steady state by the controller to achieve offset-free tracking performance. The MPC also maintains system operation within input and output constraints. Finally, the design presented here uses only temperature measurements typically available in production VCSs.

NOMENCLATURE

k	discrete time index	x	dynamic state	**Subscript**		p	performance output
r	reference (setpoint)	y	output	c	constrained output	pr	prediction model
Ts	sample time			e	estimator model	r	reference
u	control input			eq	equilibrium	u	control input
w	auxiliary state			m	measured output		

REFERENCES

Alleyne, A. (2012). Thermosys 4 toolbox. University of Illinois at Urbana-Champaign. http://arg.mechse.illinois.edu/thermosys/.

Amano, K. (2012). Heat pump apparatus and control method thereof. EP Patent App. EP20,110,007,843.

Di Cairano, S. and Bemporad, A. (2010). Model predictive control tuning by controller matching. *Automatic Control, IEEE Transactions on*, 55(1):185–190.

Di Cairano, S., Brand, M., and Bortoff, S. A. (2013a). Projection-free parallel quadratic programming for linear model predictive control. *International Journal of Control*, 86(8):1367–1385.

Di Cairano, S., Pascucci, C. A., and Bemporad, A. (2012). The rendezvous dynamics under linear quadratic optimal control. In *Proceedings of the 51st IEEE Conference on Decision and Control*, pages 6554–6559. IEEE.

Di Cairano, S., Tseng, H. E., Bernardini, D., and Bemporad, A. (2013b). Vehicle yaw stability control by coordinated active front steering and differential braking in the tire sideslip angles domain. *Control Systems Technology, IEEE Transactions on*, 21(4):1236–1248.

Elliott, M. S. and Rasmussen, B. P. (2008). Model-based predictive control of a multi-evaporator vapor compression cooling cycle. In *Proceedings of the American Control Conference*, pages 1463–1468.

Garcia, C. E., Prett, D. M., and Morari, M. (1989). Model predictive control: theory and practice—a survey. *Automatica*, 25(3):335–348.

Koeln, J. P. and Alleyne, A. G. (2013). Decentralized controller analysis and design for multi-evaporator vapor compression systems. In *Proceedings of the American Control Conference*, pages 437–442.

Maeder, U., Borrelli, F., and Morari, M. (2009). Linear offset-free model predictive control. *Automatica*, 45(10):2214–2222.

Pannocchia, G. and Rawlings, J. B. (2003). Disturbance models for offset-free model-predictive control. *AIChE Journal*, 49(2):426–437.

Simon, D. (2006). *Optimal state estimation: Kalman, H infinity, and nonlinear approaches*. John Wiley & Sons.

Skogestad, S. and Postlethwaite, I. (2005). *Multivariable Feedback Control: Analysis and Design*. John Wiley and Sons Ltd.

Wallace, M., Das, B., Mhaskar, P., House, J., and Salsbury, T. (2012). Offset-free model predictive control of a vapor compression cycle. *Journal of Process Control*, 22(7):1374–1386.

APPENDIX

Here we provide the reader with a proof guaranteeing local asymptotic stability of the MPC described in Section 3. We will make use of the prediction model, Eq. (8), rewritten in the following form,

$$\begin{bmatrix}\xi(k+1)\\ r(k+1)\end{bmatrix} = \begin{bmatrix}A_\xi & 0\\ 0 & A_r\end{bmatrix}\begin{bmatrix}\xi(k)\\ r(k)\end{bmatrix} + \begin{bmatrix}B_\xi\\ 0\end{bmatrix}\bar{u}(k) \tag{11a}$$

$$\bar{y}(k) = \begin{bmatrix}C_\xi & 0\end{bmatrix}\begin{bmatrix}\xi(k)\\ r(k)\end{bmatrix} + D_\xi\bar{u}(k) \tag{11b}$$

$$\bar{z}(k) = \begin{bmatrix}E_\xi & -E_r\end{bmatrix}\begin{bmatrix}\xi(k)\\ r(k)\end{bmatrix}, \tag{11c}$$

where $\xi(k) = \begin{bmatrix}x(k)' & w(k)' & x_u(k)'\end{bmatrix}'$, $r(k) = x_r(k)$, and $\bar{z}(k) = z(k)$.

Consider the MPC finite horizon optimal control problem

$$\min_{\bar{U}(t)} \quad \left\| \begin{bmatrix} \xi(N) \\ r(N) \end{bmatrix} \right\|_P^2 + \sum_{k=0}^{N-1} \|\bar{z}(k|t)\|_{Q_z}^2 + \|\bar{u}(k|t)\|_R^2 \tag{12a}$$

$$\text{s.t.} \quad \bar{y}_{\min} \le \bar{y}(k|t) \le \bar{y}_{\max}, \quad k = 0, \dots, N_c \tag{12b}$$

$$\bar{u}_{\min} \le \bar{u}(k|t) \le \bar{u}_{\max}, \quad k = 1, \dots, N_u \tag{12c}$$

$$\bar{u}(k|t) = K \begin{bmatrix} \xi(k|t) \\ r(k|t) \end{bmatrix}, \quad k = N_u, \dots, N-1 \tag{12d}$$

where the objective is to design the terminal cost weight P and the terminal gain K such that the tracking error is locally asymptotically stable. In order to do this we apply with some modifications the results in Di Cairano et al. (2012). In details from (11a) and (11c), we construct the system

$$\bar{x}(k+1) = \bar{A}_{pr}\bar{x}(k) + \bar{B}_{pr}\bar{u}(k) \tag{13a}$$

$$\bar{z}(k) = \bar{E}_{pr}\bar{x}(k), \tag{13b}$$

where $\bar{x} = \begin{bmatrix} \xi \\ r \end{bmatrix}$, $\bar{A}_{pr} = \begin{bmatrix} A_\xi & 0 \\ 0 & A_r \end{bmatrix}$, $\bar{B}_{pr} = \begin{bmatrix} B_\xi \\ 0 \end{bmatrix}$, and $\bar{E}_{pr} = \begin{bmatrix} E_\xi & -E_r \end{bmatrix}$. Note that (13) is not fully observable and not fully controllable because the controller cannot, in general, modify the reference, and the optimal cost does not depend on the absolute reference and output values but only on their difference. Therefore, a standard terminal cost design based on LQR fails for this system. We apply an observability decomposition via an appropriate change of coordinates T such that $x_{obs} = Tx, \quad x_{obs} = \begin{bmatrix} x_o' & x_{no}' \end{bmatrix}'$, and

$$x_{obs}(k+1) = \begin{bmatrix} A_o & 0 \\ A_{no,o} & A_{no} \end{bmatrix} \begin{bmatrix} x_o(k) \\ x_{no}(k) \end{bmatrix} + \begin{bmatrix} B_o \\ B_{no} \end{bmatrix} u(k) \tag{14a}$$

$$z(k) = \begin{bmatrix} E_o & 0 \end{bmatrix} \begin{bmatrix} x_o(k) \\ x_{no}(k) \end{bmatrix}, \tag{14b}$$

where x_{no} are the coordinates of the state vector with respect to a basis of the unobservable space, and the pair (A_o, E_o) is observable.

Theorem 1 *Let* $K = \begin{bmatrix} K_o & 0 \end{bmatrix} T$ *and* $P = T' \begin{bmatrix} P_o & 0 \\ 0 & 0 \end{bmatrix} T$ *where*

$$K_o = -(B_o' P_o B_o + R)^{-1} B_o' P_o A_o \tag{15}$$

and P_o *is the solution of the Riccati equation*

$$P_o = E_o' Q_z E_o + A_o' P_o A_o - A_o' P_o B_o (B_o' P_o B_o + R_o)^{-1} B_o' P_o A_o \tag{16}$$

which is assumed to exist. Then, the MPC controller that solves Eq. (12) *ensures that* $\lim_t \|z(t)\| = 0$*, and the tracking error* $z(t)$ *is locally asymptotically stable. Furthermore, if* A_ξ*,* A_r *do not share unstable eigenvalues such that the eigenvectors images through* E_ξ*, and* E_r *share a subspace, there exists* $\xi_{eq} \in \mathbb{R}^{\dim(A_\xi)}$ *with* $\|\xi_{eq}\| < \infty$ *such that* $\lim_t \|\xi(t) - \xi_{eq}\| = 0$*.*

Proof 1 *(Sketch) The tracking problem, Eq.* (12)*, is equivalent to a rendezvous problem of a controlled system, the plant, and an uncontrollable system, the reference. In Di Cairano et al. (2012) it was shown that the solution of the LQ problem for the observable subsystem, Eqs.* (15),(16)*, is optimal for the rendezvous problem which is non-observable. Thus, K, P are optimal for the observable system LQ problem and asymptotically stabilize the observable component of the system state, and hence the tracking error, which is related to such observable component by Eq.* (14b)*. When the MPC cost function, Eq.* (12a)*, and terminal control law, Eq.* (12d)*, are defined by K, P, the MPC behaves as the LQ-optimal controller, for all* $\bar{x} \in O^\infty(\bar{A}_{pr} + \bar{B}_{pr}K)$*, which is the maximum output admissible set of* $(\bar{A}_{pr} + \bar{B}_{pr}K)$*, subject to its constraints,Eqs.* (12c),(12b)*. Thus, the first claim is proved. The second claim is proved by exploiting the results of Di Cairano et al. (2012). The zero dynamics (i.e., the dynamics when the output, which here is the tracking error, is constantly zero) is equal to the residual dynamics after rendezvous, which is determined by the common eigenvalues with associated eigenvectors having common image through the respective output matrices,* E_ξ*,* E_r*. If there are not such unstable eigenvalues, then the state of the system is bounded.* □